Title: Time-Frequency analysis of neuronal populations with instantaneous resolution based on Noise-Assisted Multivariate Empirical Mode Decomposition

Author: Alegre-Cortés J Soto-Sánchez C Pizá ÁG Albarracín AL Farfán FD Felice CJ Fernández E

PII: S0165-0270(16)30024-3
DOI: http://dx.doi.org/doi:10.1016/j.jneumeth.2016.03.018
Reference: NSM 7486

To appear in: *Journal of Neuroscience Methods*

Received date: 11-12-2015
Revised date: 21-3-2016
Accepted date: 28-3-2016

Please cite this article as: Alegre-Cortés J, Soto-Sánchez C, ÁG Pizá, Albarracín AL, Farfán FD, Felice CJ, Fernández E.Time-Frequency analysis of neuronal populations with instantaneous resolution based on Noise-Assisted Multivariate Empirical Mode Decomposition.*Journal of Neuroscience Methods* http://dx.doi.org/10.1016/j.jneumeth.2016.03.018

Time-Frequency analysis of neuronal populations with instantaneous resolution based on Noise-Assisted Multivariate Empirical Mode Decomposition

Alegre-Cortés J[a], Soto-Sánchez C[a,b], Pizá ÁG[c,d], Albarracín AL[c,d], Farfán FD[c,d], Felice CJ[c,d] and Fernández E[a,b*] e.fernandez@umh.es

[a] Bioengineering Institute, Miguel Hernández University (UMH), Alicante, Spain
[2] Biomedical Research Networking center in Bioengineering, Biomaterials and Nanomedicine (CIBER-BBN), Zaragoza, Spain
[c] Laboratorio de Medios e Interfases (LAMEIN), Departamento de Bioingeniería, Facultad de Ciencias Exactas y Tecnología,Universidad Nacional de Tucumán, Tucumán, Argentina.
[d] Instituto Superior de Investigaciones Biológicas (INSIBIO), Consejo Nacional de Investigaciones Científicas y Técnicas (CONICET), Tucumán, Argentina.

***Address all correspondence to:**

Universidad Miguel Hernández, Instituto de Bioingeniería, Elche 03202, Spain. Tel.: +34 96522 2001.

HIGHLIGHTS

- We proposed Noise Asisted Multivariate Empirical Mode Decomposition plus Hilbert Transform as a tool to analyze neuronal population recordings.
- The method does not need any template and achieves instantaneous resolutions.
- The method was compared with previous analysis related to vibrissal tactile discrimination.
- The method was proposed to analyze nonlinear dynamics of visual cortex neuronal populations.
- The method here proposed can be adapted to many other features of biological responses.

Abstract

***Background**:* Linear analysis has classically provided powerful tools for understanding the behavior of neural populations, but the neuron responses to real-world stimulation are nonlinear under some conditions, and many neuronal components demonstrate strong nonlinear behavior. In spite of this, temporal and frequency dynamics of neural populations to sensory stimulation have been usually analyzed with linear approaches.

***New method**:* In this paper, we propose the use of Noise-Assisted Multivariate Empirical Mode Decomposition (NA-MEMD), a data-driven template-free algorithm, plus the Hilbert Transform as a suitable tool for analyzing population oscillatory dynamics in a multi-dimensional space with instantaneous frequency (IF) resolution.

***Results**:* The proposed approach was able to extract oscillatory information of neurophysiological data of deep vibrissal nerve and visual cortex multiunit recordings that were not evidenced using linear approaches with fixed bases such as the Fourier analysis.

***Comparison with existing methods**:* Texture discrimination analysis performance was increased when Noise-Assisted Multivariate Empirical Mode plus Hilbert Transform was implemented, compared to linear techniques. Cortical oscillatory population activity was analyzed with precise Time-Frequency resolution. Similarly, NA-MEMD provided increased Time-Frequency resolution of cortical oscillatory population activity.

***Conclusions**:* Noise-Assisted Multivariate Empirical Mode Decomposition plus Hilbert Transform is an improved method to analyze neuronal population oscillatory dynamics overcoming linear and stationary assumptions of classical methods.

Keywords

NA-MEMD, nonlinear analysis, non-stationary analysis, neuronal population.

1 INTRODUCTION

Biological signal analysis has been historically limited due to nonlinearity and non-stationarity of the data. In particular, the nervous system detects and processes world information continuously through highly complex dynamics from peripheral nerves to the cortex (Averbeck et al. 2006; Bathellier et al. 2008; Safaai et al. 2013) at very different time scales (Theunissen and Miller 1995; Buonomano and Maass 2009; Klampfl et al. 2012). A common example is the production of action potentials by a neuron, where the output signal has no simple linear relationship to the input. However, the development of general methods for analyzing nonlinear systems and interpreting the results has been delayed due to the theoretical and computational complexities involved.

In this paper we propose the use of Noise-Assisted Multivariate Empirical Mode Decomposition (NA-MEMD) (Mandic et al. 2013) together with Hilbert Transform (Huang et al. 1998) as a tool for the study of neuronal population dynamics with high temporal resolution. Multivariate Empirical Mode Decomposition (MEMD) (Rehman and Mandic 2010) was proposed as a n-dimensional extension of empirical mode decomposition (EMD) (Huang et al. 1998). This is an empirical adaptive method which iteratively subtracts the mean vector obtained from binding the local maxima and minima with a cubic spline until a certain criterion is satisfied. The result of this algorithm is a variable number of Intrinsic Mode Functions (IMFs) that contains the existent data oscillations in decreasing frequency order. The extension to n-dimensions of this method described in Rehman and Mandic 2010, is based on real-valued projections along multiple directions on hyperspheres, in order to calculate the envelopes and the local mean of multivariate data. Furthermore, the addition of new dimensions containing white Gaussian noise (NA-MEMD) (Rehman and Mandic 2011) acts as a filter bank that helps to resolve the mode mixing and mode misalignment problem present in MEMD algorithms. In addition, the additional number of extrema provided by noise channels confers an increase in accuracy when intermittent signals are decomposed, which is crucial when leading with neuronal population dynamics.

EMD family of algorithms has recently been applied to discriminate between whole LFPs of macaque V4 while performing a visual illusion task without specifically considering neuronal dynamics via EMD (Liang et al. 2005a, 2005b) and MEMD (Hu and Liang 2011, 2012). In addition, EMDs have been used successfully to analyze EEG and EMG recordings (Huang et al. 2013; Al-Subari et al. 2015; Naik et al. 2015) in the last years. Bearing this in mind, we aim to explore the potential usefulness of this methodology for describing and understanding local neuronal population recordings with precise instantaneous temporal resolution.

In this paper we describe the implementation of the technique and then apply it on to real data. In particular, we show how neural activity oscillatory activity changes in two different experimental paradigms: evoked activity recorded from the deep vibrissal

nerve of anesthetized rats and spike trains of simultaneously recorded neurons from deep layers of rat visual cortex. Our results suggest that NA-MEMD plus Hilbert transform analysis is a improved tool to study local neuronal activity with instantaneous time and frequency resolution, consistently with recent works (Hu and Liang 2014) where NA-MEMD decomposition plus Wasserstein distance based analysis of LFP recordings increased whole recordings discrimination accuracy.

2 METHODS

2.1 Experimental methods

2.1.1 Electrophysiological recordings

Deep vibrissal nerve recordings were obtained from five male Wistar adult rats weighing 300–350 g. Surgical anesthesia was induced by urethane (1.5 g/kg) and temperature was maintained at 37° by a servo-controlled heating pad. Surgery and experimental protocol have been previously described in detail by Albarracín et al., 2006. The procedures are briefly described below. Vibrissa movements were induced by electrical stimulation of facial motor nerve (VII). Square-wave pulses (30 μs, 7 V supramaximal, 5 Hz) simulated vibrissal whisking at its natural frequency (Fig. 1A). Nerve activity was recorded and digitized at 20 kHz (sampling rate) during a 100 ms window following onset of each cycle of whisker movement with a Digidata 1322A (Axon Instruments). Fifty whisker movement cycles were obtained for each whisker-surface contact, and an additional 50 cycles were recorded while whisker moved unobstructed in air (control).

Four slip-resistance levels were presented for each surface by mounting the surface at different distances from the whisker base (Fig. 1A, Albarracín et al. 2006, for details). The swept surfaces tested in this paper were surfaces with different textures: wood, metal, acrylic and sandpaper P1000. Movements of the Gamma whisker were recorded simultaneously with nerve activity using a custom-made photoresistive sensor (Dürig et al. 2009). The frequency response of the sensor was maximal in the range 0–100 Hz, enabling direct identification of the protraction and retraction phases of the movement cycle.

Visual cortex multi-unit recordings were obtained from 5 male Long Evans adult rats weighing 450-500 gr. Analgesia was induced by buprenorphine (0.025mg kg-1 s.c), and surgical anesthesia and sedation were induced by ketamine HCl (40 mg kg-1 i.p). The anesthesia was maintained with a mix of oxygen and 2% of isoflurane during the surgery and afterwards reduced to 1.5% during the electrophysiological recordings. The blinking and the toe pinch reflexes were continuously checked along the experiment to guarantee a proper level of anesthesia for the animal. The body temperature was maintained with a thermal pad and the heart rate and O2 concentration in blood were monitored throughout the experiment. Animals were pre-treated with dexamethasone (1

mg kg^{-1} i.p) 24 hours and 20 minutes prior to surgery in order to avoid brain edema caused by the electrode insertion. A craniotomy was drilled on top of the visual cortex and the electrode array was inserted 2 mm lateral to the midline and from 0.5 mm anterior to lambda. Then, a Utah array was inserted in the deep layers of the visual cortex (>600 µm) with a Blackrock pneumatically-actuated inserter device specifically designed for implanting the Utah array through the duramatter with a minimal tissue offense (Blackrock Microsystems, Salt Lake City, USA). The customized microelectrode Utah array consisted of 6 x 6 tungsten microneedles, covering a brain surface of 2 mm x 2 mm millimeters (400 µm spacing). After the insertion, the ipsilateral eyelid to the craniotomy site was closed with cyanoacrylate and atropine sulphate 1% was used to -dilate the pupil of the contraleral eye.

In vivo neural activity from visual cortex was recorded simultaneously from 16 individual electrodes with the Utah array (Fig 2A). The Utah array was connected to a MPA32I amplifier (Multichannel Systems, MCS) and the extracellular recordings were digitized with a MCS analog-to-digital board. The data were sampled at a frequency of 20 kHz and slow waves were digitally filtered out (100-3000 Hz, 2^{nd} order Butterworth type IIR digital filter) from the raw data (Fig 2B). Neural spike events were extracted with a free-tool application for offline spike sorting analysis (Neural Sorter, http://sourceforge.net/projects/neuralsorter/) and the resulting multiunit information obtained from each electrode was stored for further analysis.

Visual stimulation consisted on a vertical drifting square-wave grating (90°, light and dark bars, 100% contrast, 6 Hz, 0.6 cycles/degree) of 500 ms duration interspersed with a dark (uniform) stimulus of equal duration. The stimulus was displayed on a LCD monitor (refresh rate 60 Hz) and a luminance of ≈100 cd/m^2, placed 25 cm in front of the right eye, approximately at 30° from the midline and covering a visual field spanning ≈100° (Fig. 2A). The stimulus was generated using the vision egg library and a python script. The room was kept in darkness throughout the visual stimulation.

2.1.2 Ethical approval

All the procedures carried out at the Institute for Biological Research (INSIBIO)/Instituto Superior de Investigaciones Biológicas, were in accordance with the recommendations of the Guide for the Care and Use of Laboratory Animals (National Research Council, NRC).

All the experimental procedures carried out at the Miguel Hernandez University were conformed to the directive 2010/63/EU of the European Parliament and of the Council, and the RD 53/2013 Spanish regulation on the protection of animals use for scientific purposes and approved by the Miguel Hernandez University Committee for Animal use in Laboratory.

2.2 Data analysis

Neural activity analysis was performed in Matlab (MathWorks). In the case of the rat visual cortex multiunit recordings, single or multiunit spiking activity was isolated from the background. We observed multiunit activity in the majority of the electrodes through the whole recording sessions, and only those electrodes with neural activity higher than 0.5 spikes/s were considered in the analysis.

We constructed time-dependent population activity vectors from rat visual cortex multiunit recordings by temporally locking the activity of each electrode with 1 ms resolution from one second before to one second after each stimulus presentation. The deep vibrissal nerve recordings remained at recording resolution (20 kHz).

2.2.1 NA-MEMD

EMDs are data-driven algorithms suitable for nonlinear and non-stationary analysis (Mandic et al. 2013); therefore, they have become a promising tool in the analysis of neural data (Liang et al. 2005a). ‘Classical’ EMD analysis (Huang et al. 1998) decomposes a given signal in a set of oscillatory modes called IMFs. Each IMF contains the oscillations present in the original data at a certain temporal scale and therefore is independent of templates. Thus this procedure provides a much more elaborate means of applying nonlinear analysis to neuronal population recordings than standard procedures.

The MEMD (Rehman and Mandic 2010) is a multivariate extension of EMD algorithm, where analysis of simultaneous dimensions is performed simultaneously to obtain a meaningful decomposition of the whole multidimensional signal, This method overcomes the problems resulting from univariate EMD analysis application to each dimension independently: different number of IMFs and unscaled alignments. It obtains generalized oscillations, known as rotational modes, via estimation of the local n-dimensional mean. To this end, multiple uniformly distributed projections in the n-dimensional space are calculated using a V-point Hammersley sequence (Niederreiter 1992); these projections extrema are interpolated with a cubic spline and averaged to compute the local mean. As in the original EMD algorithm (Huang et al. 1998), this mean vector is subtracted from the original n-dimensional data and the process is repeated iteratively to obtain the subsequent IMFs until a certain stopping criteria is achieved, such as symmetry of the upper and lower envelopes or that the number of extrema and the number of zero-crossings differ at most by 1. The final IMF does not contain any oscillation other than the trend of the data.

Whereas complete MEMD algorithm is described elsewhere (Rehman and Mandic 2010), Algorithm 1, as given in this paper, briefly describes for those unfamiliar with the technique, the basis of the method:

Algorithm 1. Multivariate extension of EMD.

1. Choose a suitable pointset for sampling on an (n −1) sphere.
2. Calculate a projection, denoted by $p^{\theta k}(t)\}_{t=1}^{T}$, of the input signal $\{\boldsymbol{v}(t)\}_{t=1}^{T}$ along the direction vector $\boldsymbol{x}^{\theta k}$, for all k (the whole set of vectors), giving $p^{\theta k}(t)\}_{t=1}^{T}$ as the set of projections.
3. Find the time instants $\{t_i^{\theta k}\}$ corresponding to the maxima of the set of projected signals $p^{\theta k}(t)\}_{t=1}^{T}$
4. Interpolate $[t_i^{\theta k}, \boldsymbol{v}(t_i^{\theta k})]$ to obtain multivariate envelope curves $\boldsymbol{e}^{\theta k}(t)\}_{k=1}^{K}$
5. For a set of K direction vectors, the mean $\boldsymbol{m}$(t) of the envelope curves is calculated as $\boldsymbol{m}(t) = \frac{1}{K}\sum_{k=1}^{K} e^{\theta k}(t)$
6. Extract the 'detail' d(t) using d(t) = x(t) - m(t). If the 'detail' d(t) fulfills the stoppage criterion for a multivariate IMF, apply the above procedure to x(t) – d(t), otherwise apply it to d(t).

White Gaussian Noise (WGN) addition to EMD analysis (EEMD, NA-MEMD) increases its performance via reducing mode mixing produced by signal intermittency (Zhaohua and Huang 2009) acting as a quasi-dyadic filter bank that enhances time-frequency resolution (Flandrin et al. 2004; Rehman and Mandic 2011). This increased performance is especially present in intermittent data, where aliasing among IMFs is more prone to happen; therefore the dyadic filter bank property of WGN decomposition helps to mitigate this effect. Given known the intermittency of neural signals, WGN is added in additional dimensions:

$$d = n + k,$$

Where *d* is the final number of dimensions, *n* the dimensions of the original data (electrodes, trials…) and *k* the number of additional dimensions including WGN (Rehman and Mandic 2011).

In order to apply NA-MEMD analysis to our data, we adapted MEMD Matlab package (http://www.commsp.ee.ic.ac.uk/~mandic/research/emd.htm). We used the low-discrepancy Hammersley sequence to generate a set of V = 300 direction vectors for computing signal projections and 3 WGN channels. Standard stopping criterion was described elsewhere (Rilling et al. 2003).

We applied NA-MEMD in different ways accordingly to each dataset. When applied to deep vibrissal nerve recordings, we extended the analysis to all repetitions (*n* = 50), obtaining *d* = 53. When studying visual cortex results, we aimed to depict features present in the whole recorded population; therefore, we averaged the activity of all electrodes and trials (*n* = 1) and added 3 additional dimensions with WGN, *d* = 4. We kept applying NA-MEMD over EEMD (Zhaohua and Huang 2009) on visual cortex recordings collapsed to a single dimension to avoid mixing the added noise with the real signal, as it may increase residual error and produce different number of IMFs in each ensemble, therefore compromising IMFs alignment and subsequent analysis (see Figs. 5 & 8 in Mandic et al. 2013).

2.2.2 Hilbert Transform

We measured present frequencies in our data as the instantaneous frequency (IF) using Hilbert Transform (Huang et al. 1998). For a given time series x(t), its Hilbert Transform H(x)(t) is defined as:

$$H(x)(t) = \frac{1}{\pi} C \int_{-\infty}^{\infty} \frac{x(t')}{t-t'} dt',$$

Where C indicates the Cauchy principal value. Hilbert Transform results in a complex sequence with a real part which is the original data and an imaginary part which is a version of the original data with a 90º phase shift; this *analytic signal* is useful to calculate instantaneous amplitude and frequency; instantaneous amplitude is the amplitude of H(x)(t), IF is the time rate of change of the instantaneous phase angle.

2.2.3 Spectrogram via short-time Fourier transform (STFT)

STFT analyzes the signal x(t) through a short-time window $\omega(t) = x(t) \times \omega(t - \tau)$, and then a Fourier transform is performed on this product using complex exponential basis functions. The square modulus of STFT is referred to as the spectrogram (Zhan et al., 2006). In order to observe overall changes in the power spectral density (PSD), we computed it using a parametric autoregressive (AR) modeling (Pardey et al. 1996; Albarracín et al. 2006) in both raw and decomposed signals.

2.2.4 Information measure with Bhattacharyya distance

The Bhattacharyya distance (Bd) is a measure of divergence between two distributions (Bhattacharyya, 1946). We measured this value to discriminate between possible pairs of experiments.

3 RESULTS

3.1 Deep vibrissal nerve recordings

The afferent discharge recorded is the average electrical activity of myelinated axons with different firing patterns (Albarracín et al., 2006; Farfán et al., 2013). This leads to a complex response to the stimulus where the individual response of each fiber is mixed in a summed response. Fig. 3A shows four afferent recordings (top) in different sweep situations and 6 IMFs obtained applying NA-MEMD analysis to each of the surfaces recordings individually. We decided to inspect all IMFs rather than statistically validate those carrying more information (Huang et al. 2013; Hu and Liang 2014) in order to understand the discrimination dynamics across time at all frequencies.

In order to observe overall changes in the power spectral density (PSD), we computed it using a parametric AR modeling (Pardey et al. 1996; Albarracín et al. 2006) in both raw and decomposed signals. The PSD of raw signals revealed differences of amplitude (power of PSDs) and in its maximum-energy frequency

components (Fig. 3B, top panel). In this analysis, both the electrical stimuli as well as EMG artifacts were dropped of PSD estimations to avoid spurious components. The Fm (mean frequency) values (Phinyomark et al. 2009) of 50 PSD of each experimental situation were represented with its mean values bounded by its corresponding standard deviations (Fig. 3C, left). Significant differences among sweep situations on metal, acrylic and sandpaper were observed, although not between sweeps on wood vs. metal (Kruskal Wallis test, p value < 0.05).

The PSD obtained from IMFs revealed spectral changes at different bandwidths (Fig. 3B). For instance, IMF 3 concentrated its energy content in the bandwidth of 1.25 to 2.5 kHz (for all sweep situations), while IMF 4 into 0.5 to 1.25 kHz approximately. Thus, the power remained increasingly bound in specific bands. The Fm values from each IMF and simulated whisking situation are represented in Fig. 3C (middle).

The spectral content of IMF 5 showed similarities with the spectral content of raw signals, regarding to the sweep situation on metal, acrylic and sandpaper, and a linear increase in Fm (Fig. 3C, right), however, results variance was notably reduced. For this IMF, the sweep on wood vs sweep on metal is significantly different ($p<0.01$, ANOVA test). The Fm values of IMF 6 showed a linear increase for sweep situations on wood, metal and acrylic. The sweep situation on sandpaper produces a spectral content characterized by Fm values of lower magnitude and dispersion compared to the PSD of the raw data (Fig. 3C, right).

Time-Frequency (T-F) discrimination analysis, as proposed by Pizá et al., 2014, was implemented in order to compare the NA-MEMD plus Hilbert transform as a method to extract time-frequency features of afferent recordings. Fig. 4A shows the methodology used to obtain a discriminability measure based on spectrograms. Each whisking situation was represented as a time series average and its corresponding standard deviation (mean ± std), in order to compare the temporal profile of different whisking situations.

Alternatively, the NA-MEMD was applied to raw signals and then the IF of selected IMFs was computed via Hilbert Transform (see methods). Therefore, we obtained T-F profiles for each whisking condition and IMF (one example condition shown in Fig. 4B). We could observe how time-frequency features of NA-MEMD plus Hilbert Transform analysis had lower dispersion than those obtained from the spectrograms (Supplementary Fig. 1).

Bd was used to compare T-F dynamics for three comparisons at three slip resistance levels, as we did not find substantial differences between slip resistances 2 & 3. Results are shown in Fig. 4C. Bd values increased in a range from 0-0.3 for comparisons based on spectrograms to 0-1.5 Bd values from Hilbert Transform of IMFs 5 & 6. Furthermore, the instantaneous T-F resolution of this procedure showed an enriched temporal dynamic of Bds. T-F analysis based on spectrogram reveals differences between wood and acrylic into the 16 to 24 ms time interval for all slip

resistance levels (Fig 4C, top – left). In the same time interval, the Hilbert Transform of IMF 5 showed a peak of discrimination at 18 ms for slip resistance 4 , and at 22 ms for slip resistance 2 (Fig. 4C, middle – left). This situation was even clearer when IMF 6 Hilbert Transform was analyzed. In addition, a different peak in the discrimination analysis (Bd> 0.5) arose at 30 ms, for slip resistance 1 (Fig. 4C, bottom – left).

When this comparative analysis was extended to the discriminations between wood and metal, maximum Bd was found in retraction phase (20 – 45 ms approx.), at slip resistance 1 (Fig. 4C, top – middle) in the Hilbert Transform of IMF 6 (200 to 500 Hz) (Fig. 4C, bottom – middle), something completely absent in the spectrogram derived T-F profile.

Finally, spectrogram method revealed that acrylic vs sandpaper comparison had its greatest discriminability value in the protraction phase (16 to 25 ms approx.) (Fig. 4C, top – right). Hilbert Transform of IMF 5 displayed peaks in the Bd in the same window, although the measured value was higher and the increased temporal resolution demonstrated that maximum Bd was displaced for different resistances (maximum Bd with resistance 4), something previously blurred by the linear approach limitations; On the other hand, Hilbert Transform of IMF 6 had a maximum at a different resistance (resistance 2) as well as a different temporal profile.

These results clearly showed the advantages of NA-MEMD plus Hilbert Transform over T-F analysis based on spectrograms, as it was used to compute higher Bds in all situations with increased time resolution. Furthermore it was possible to differentiate the time of maximum Bd for different texture pairs.

3.2 Visual cortex recordings

Neurons of mammals neocortex oscillate spontaneously (Buzsáki and Draguhn 2004; Petersen et al. 2003; Luczak et al. 2007), both in awake and anesthetized states (Haider et al. 2007; Luczak et al. 2007) although alternate with some periods of desynchronized activity (Okun et al. 2013). In this conceptual framework, we have to take into account that the visual cortex neuronal populations recorded during visual stimulation may have different coupling among neurons. Thus, whereas some neurons fire independently others fire simultaneously in population oscillations (Okun et al. 2015) resulting in a strong variability in the population responses (Carandini 2004).

To analyze these data we averaged the spiking activity of the whole recorded population during visual stimulation and decomposed it with NA-MEMD. Fig. 5A shows the mean population response to a single trial (left) and two IMFs, one carrying information about the distribution of single spikes (IMF3, center) and the other about the low frequency oscillation (IMF7, right). IF (Fig. 5B) of the data shown in Fig. 5A is computed via Hilbert Transform and shows how IF vector of the original data (left) is artefactual, while center and right graphs show the IFs of the IMFs shown above and how they are restricted to a certain frequency range. It is especially notorious how NA-MEMD plus Hilbert Transform allowed to analyze intrawave oscillations (Figs. 5A&

5B, right), something which is not feasible by using linear techniques. Figs. 5C & 5D show the same scheme explained in the top part of Figs. 5A & 5B extended to the whole experiment averaged in a single vector. This was performed averaging the activity of all electrodes and trials. Note how IMF 3, containing high frequency components of the response is not stimulus-dependent, while IMF 7, containing low frequency oscillations (±10 Hz, see right graph of Fig. 5D) is amplitude-modulated (AM) during the stimulation window (grey window). These results are consistent with the interpretation that the distribution of spikes is highly variable in response to each stimulation (IMF 3). This methodology also allows to discover oscillations in a different time-scale (IMF 7), which could be related to the stimulus (Druckmann and Chklovskii 2012).

In order to compare this analysis with traditional linear approach, we constructed averaged spiking activity power spectrums using spectrogram and NA-MEMD plus Hilbert Transform analysis independently (Fig. 6). Hilbert spectrum time resolution was increased, as it was obtained from a point-by-point convolution instead of windows superposition spectrogram analysis. Moreover, when Fig. 6C and Fig. 6D are compared, we can notice an increase in frequency resolution in Hilbert spectrum, whereas spectrogram frequency axis is blurred and lacks of the resolution achieved in Hilbert spectrum. When an accurate representation of nonlinear features is analyzed, we can observe how a power peak with a linear increase in frequency appears between 250 and 350 ms after stimulation onset and 35 and 45 Hz in Fig. 6D, computed with NA-MEMD plus Hilbert Transform, but is absent in Fig. 6C spectrogram, which was unable to depict this frequency increase along time due to its template restrictions.

In conclusion, NA-MEMD plus Hilbert Transform provided an enriched spectrum when compared with traditional techniques (spectrogram), with increased T-F resolution and a template-free representation of nonlinear response components, thanks to its template-free, local application. Thus, a T-F analysis of dynamical properties of multielectrode visual cortex recordings with IF resolution is feasible with NA-MEMD plus Hilbert transform.

4 Discussion

The present results were obtained using NA-MEMD plus Hilbert Transform, an approach that enabled the study of population dynamics with instantaneous resolution. The absence of any fixed basis in the decomposition increased the accuracy of the analysis and avoided the T-F blurring of linear approaches. When linear or stationary assumptions are used, intrawave modulations result in spurious harmonics residing in higher frequencies that obscure the biological interpretation of the results. As neuronal dynamics are classically nonlinear (Laurent 1996; Shamir 2004; Averbeck et al. 2006), we suggest that nonlinear techniques are required for a more confident and meaningful analysis of neuronal data.

The EMD family of algorithms has been used in the recent years in neuroscience to overcome these difficulties (Liang et al. 2005b; Hu and Liang 2011, 2012, 2014, Naik et al. 2015). In the present study we have demonstrated that NA-MEMD, a noise-assisted data-driven Time-Frequency analysis algorithm, is a suitable tool to study local neuronal populations. Our results show that this approach may be useful to dramatically increase the time resolution of Time-Frequency analysis of neuronal population recordings.

Instantaneous frequency resolution is essential for a meaningful interpretation of nonlinear and non-stationary processes (Durstewitz and Deco 2008). Thus, by using the procedure described in the present study we have been able to show how afferent population activity presents intrawave frequency modulations (see Supplementary Fig. 2). Previous attempts were unavailable to achieve such temporal resolution in T-F analysis (Albarracín et al., 2006; Farfán et al., 2013), and blurred the information obtained. Thus, linear Fm analysis of the deep vibrissal nerve recordings used in those studies were not able to accurately explain the nerve responses to vibrissal stimulation, something fulfilled when using NA-MEMD plus HT analysis (see Fig. 4 and Supplementary Fig 1). Hence it is possible that those previous analysis may contain significant artifacts, what emphasizes the usefulness of this new approach to extract time-frequency information from neural recordings.

In addition, this procedure was also applied to visual cortex simultaneous multiunit recordings. To the best of our knowledge, this is the first attempt of extracting oscillatory information from spiking activity using NA-MEMD analysis. Our T-F analysis of mean population activity evidenced intrawave modulations before, during and after stimulation, with a power peak that started at 35 Hz and increased to 45 Hz lasting approximately 200 ms in the response window (Fig. 6D). This response feature was nonlinear, as it changed in time and frequency simultaneously, therefore spectrogram analysis was not able to accurately depict it (Fig. 6C). Further analysis of neuronal populations oscillatory response to stimulation at different time-scales will be addressed in future studies

5 Conclusions

We have shown how NA-MEMD analysis, a noise-assisted nonlinear non-stationary template free approach, extracts monocomponent oscillatory information of neurophysiological recordings from deep vibrissal nerve and improves previous discrimination analysis using Bhattacharyya distance with enhanced temporal resolution. Moreover, we used NA-MEMD to extract oscillatory components from population multielectrode spiking recordings of rat visual cortex while visually stimulated and obtained oscillatory components related to cortical response in order to describe it with instantaneous T-F resolution. We compared these results with

spectrogram analysis and showed how T-F resolution was strongly increased, and how nonlinear response features were obtained with increased accurancy.

We propose to extend NA-MEMD analysis to oscillatory dynamics of neuronal populations to solve the problem of facing nonlinearity and non-stationarity when studying the data, as it has already been doing on certain high-scale experimental paradigms (EEG/EMG/LFP, Huang et al. 2013; Al-Subari et al. 2015; Naik et al. 2015, Hu and Liang 2014). The instantaneous resolution achieved in both frequency and time domains, as well as the noise-removal capability demonstrated by this algorithm may open a new field in any kind of neural analysis.

Acknowledgements

We thank Lucas J. Morales Moya for his helpful advice in NA-MEMD implementation.

This work has been supported in part by grant MAT2012-39290-C02-01 from the Spanish Government, by the Bidons Egara Research Chair of the University Miguel Hernández, by a research grant of the Spanish Blind Organization (ONCE) and by grants from Agencia Nacional de Promoción Científica y Tecnológica (ANPCYT) PICT 2012-1210; Consejo Nacional de Investigaciones Científicas y Técnicas (CON-ICET), Consejo de Investigaciones de la Universidad Nacional de Tucumán (CIUNT) E532 and Institutional funds from Instituto Superior de Investigaciones Biológicas (INSIBIO).

FIGURES

Figure 1

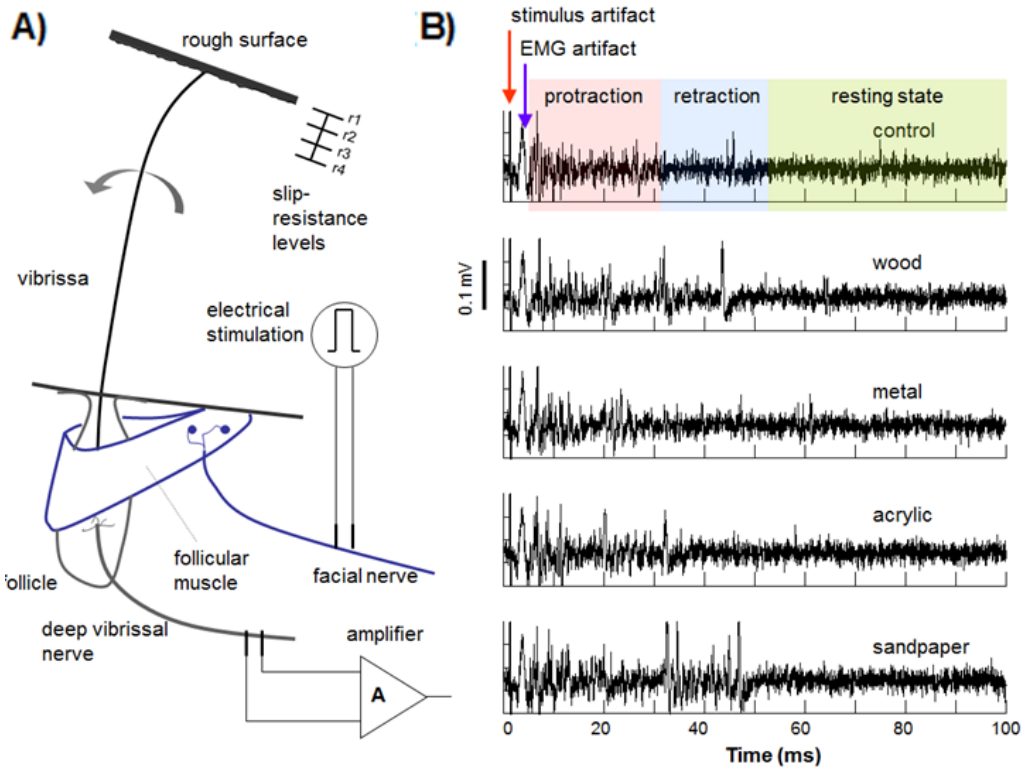

Fig. 1 Schematic representation of the experimental stimulus-recording design. A) The facial nerve is stimulated to induce the artificial movement of the vibrissa. Rough surfaces are faced to vibrissal movement to force contact during movement with controlled pressure while afferent activity is recorded. B) Afferent activity recordings obtained in five sweep situations: air sweep (control), sweep on wood, sweep on metal, sweep on acrylic and sweep on sandpaper P1000. All activity recordings were obtained at slip-resistance 4. Stimulus artifact and an artifact due to EMG volume conduction are observed. Protraction, retraction and resting phases are identified (Albarracín et al, 2006).

Figure 2

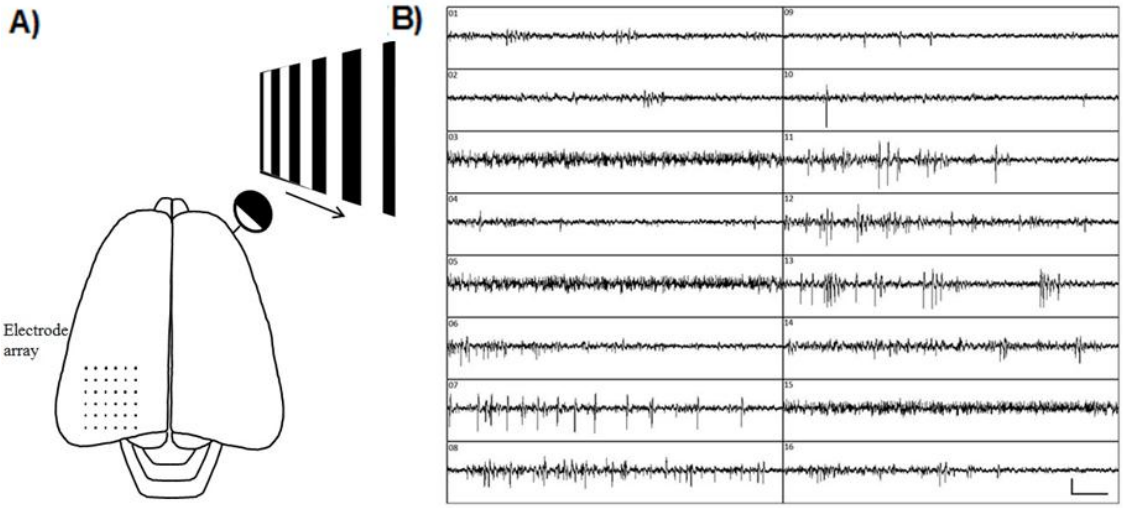

Fig. 2 A) Schematic representation of the experimental stimulus-recording design. B) Screen capture showing the display of the extracellular recording from 16 electrodes simultaneously. Each panel in the image corresponds to an individual electrode of the array. Scale bar in the last bottom panel corresponds to 150 μV in the vertical axis and 50 ms in the horizontal axis.

Figure 3

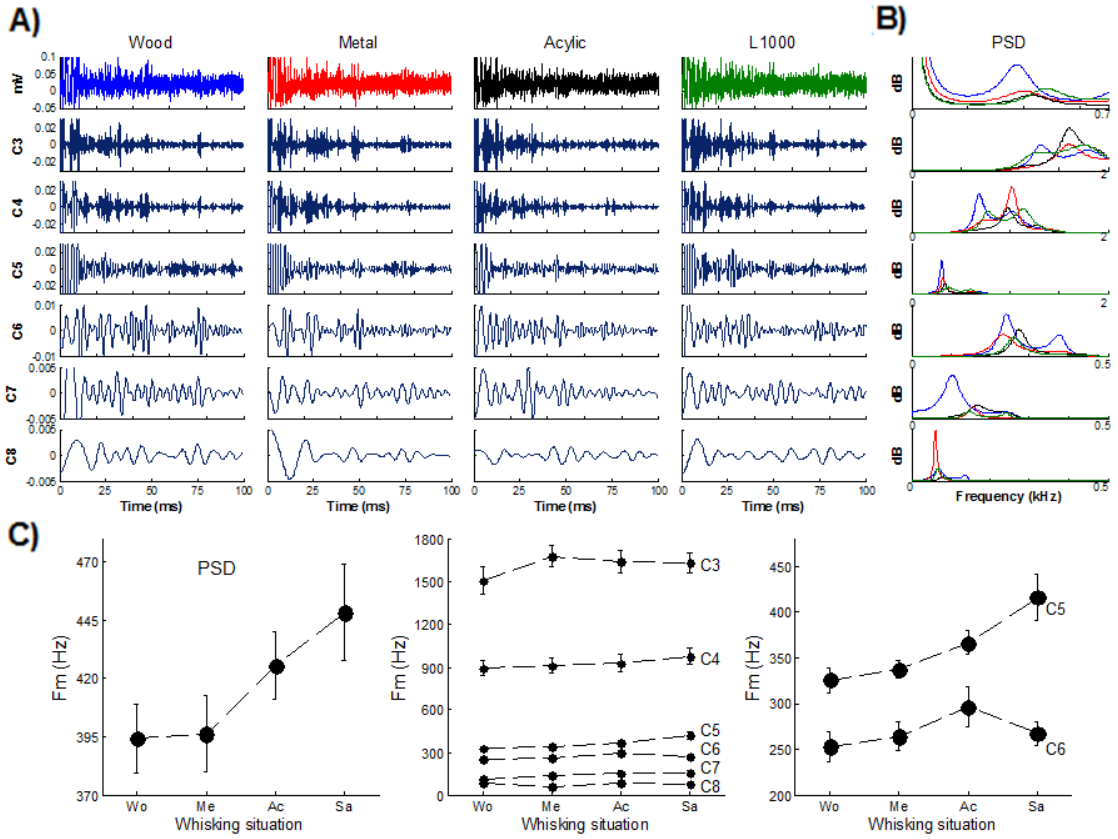

Fig. 3 Spectral analysis using power spectral density (PSD) and noise-assisted empirical mode decomposition (NA-MEMD). (A) NA-MEMD analysis of four afferent activity recordings evoked by sweep on wood (blue), metal (red), acrylic (black) and on sandpaper P1000 (L1000, green). All activity recordings were obtained at slip-resistance. The 3rd to 8th intrinsic mode functions (IMF) from each afferent recording and IMFs for each whisking situation are shown. B) PSDs computed using the Burg parametric estimation method (Albarracín et al. 2006) for each whisking situation. C) PSD represented by its mean spectral frequency (Fm). Left, fifty Fm values were obtained for each experimental situation. For raw data, Fm values within the range of 100 to 600 Hz were obtained. Middle, Fm values from IMFs were obtained within its corresponding bandwidth. Right, Fm values from C5 and C6 modes for each whisking situation.

Figure 4

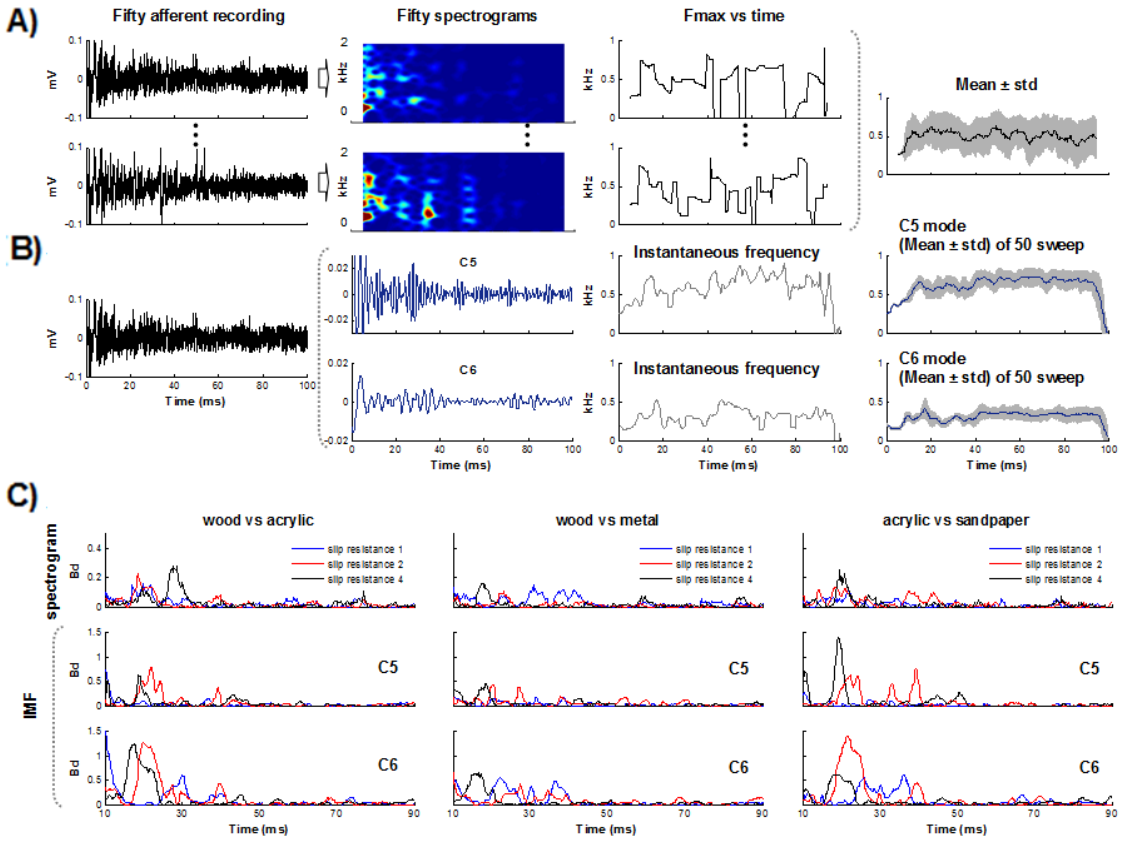

Fig. 4 Time-frequency analysis from spectrogram, NA-MEMD and Hilbert spectral methods. A) Spectrogram method. Fifty spectrograms were obtained from fifty afferent recordings for one experimental situation. Then, maximum energy components (Fmax) into frequency range of 10–1000 Hz were obtained for each spectrogram along time. Thus, a mean ± std of Fmax values along time is obtained. B) NA-MEMD and Hilbert spectral method. Each afferent recording is subjected to the empirical decomposition, and a Hilbert transform is applied to each IMF to obtain de instantaneous frequency along time (time-frequency information). C) Comparisons and discriminability measure. A discriminability measure was obtained by using Bhattacharyya distance (Bd).

Figure 5

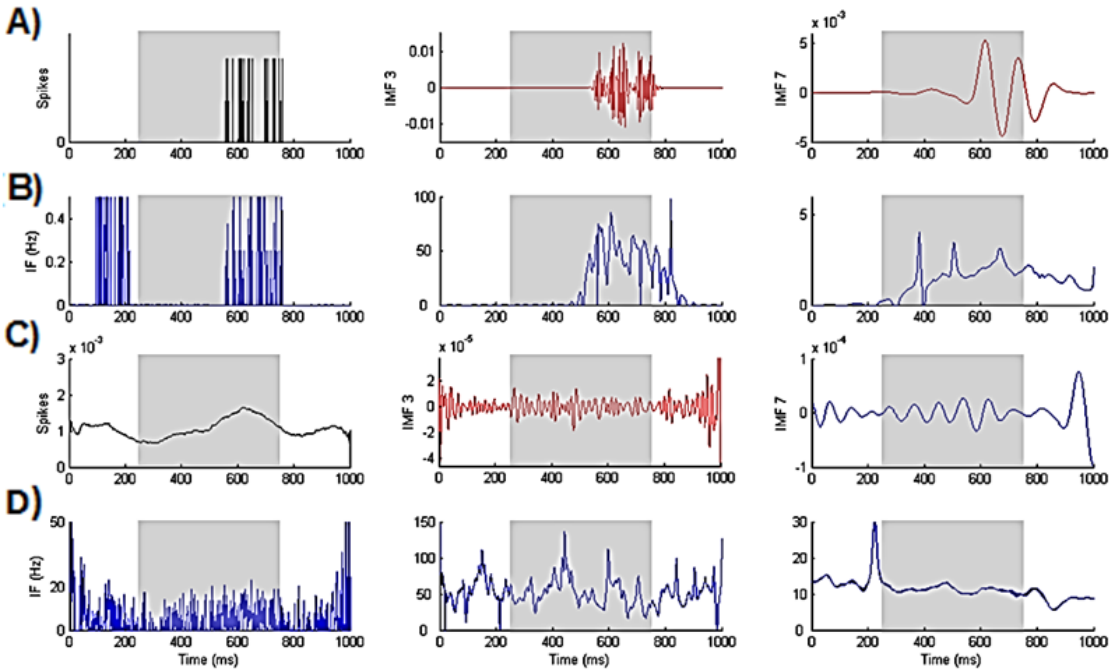

Fig. 5 Time frequency analysis from single trial and mean activity vectors. A) Left, single trial mean population activity; center, IMF 3, containing high frequency (±50 Hz) oscillations; right, IMF7 containing low frequency (±2 Hz) oscillations. B) Instantaneous frequency from graphs in A) calculated with Hilbert transform. C) Left, mean population activity for all electrodes and trials; center, IMF 3, containing high frequency (±50 Hz) oscillations; right, IMF7 containing low frequency (±10 Hz) oscillations. D) Instantaneous frequency from graphs in C) calculated with Hilbert Transform. Stimulus represented as a grey shaded rectangle.

Figure 6

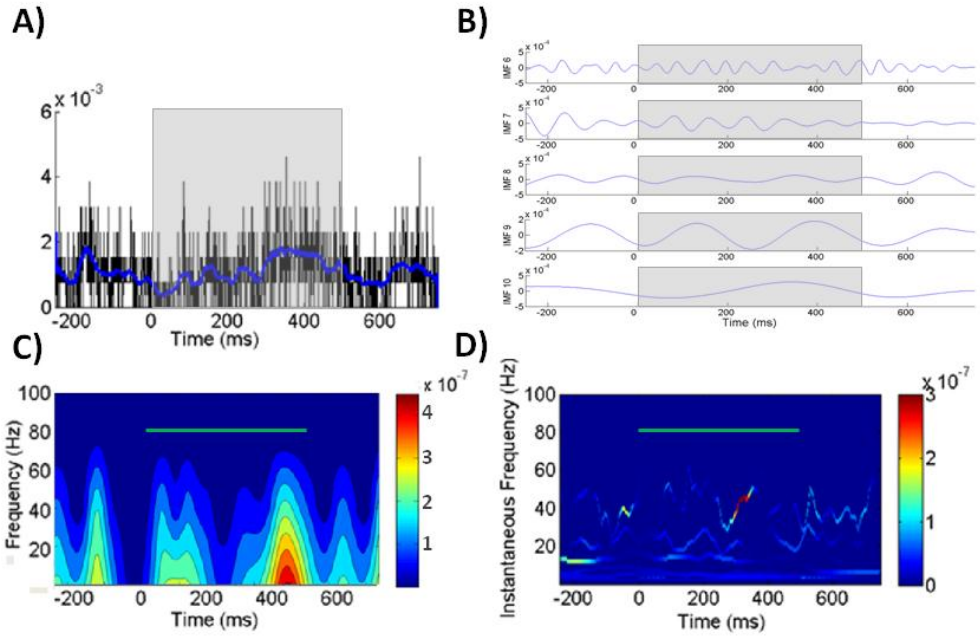

Fig. 6 A) Mean population activity during visual stimulation, mean activity smoothed with a 30 ms window displayed in blue color for easier visualization. B) Resulting IMFs from 6 to 10 after NA-MEMD decomposition. C) Spectrogram of mean population activity data. D) Hilbert Spectrum of IMFs 6 to 10. An increase in temporal resolution and power locking is observed. Stimulus represented as a grey shaded rectangle in A) & B) and a green horizontal bar in C) & D).

6 REFERENCES

Albarracín AL, Farfán FD, Felice CJ, Décima EE. Texture discrimination and multi-unit recording in the rat vibrissal nerve. BMC Neurosci. 2006;7-42. DOI: 10.1186/1471-2202-7-42

Al-Fahoum AS, Al-Fraihat AA. Methods of EEG Signal Features Extraction Using Linear Analysis in Frequency and Time-Frequency Domains. ISRN Neurosci. 2014; 1-7. DOI: 10.1155/2014/730218

Al-Subari K Al-Baddai S, Tomé AM, Goldhacker M, Faltermeier R, Lang EW. EMDLAB : a toolbox for analysis of single-trial EEG dynamics using empirical mode decompostion. J Neurosci Methods. 2015;253:1-14. DOI: 10.1016/j.jneumeth.2015.06.020

Averbeck BB, Latham PE, Pouget A. Neural correlations, population coding and computation. Nat Rev Neurosci 2006;7(5):358–66. DOI: 10.1038/nrn1888

Bathellier B, Buhl DL, Accolla R, Carleton A. Dynamic ensemble odor coding in the mammalian olfactory bulb: sensory information at different timescales. Neuron 2008;57(4):586–98. DOI: 10.1016/j.neuron.2008.02.011

Bhattacharyya A. On a measure of divergence between two multinominal populations. Sankhyā: The Indian Journal of Statistics (1933-1960) 1946; 7(4):401–6

Buonomano D V, Maass W. State-dependent computations: spatiotemporal processing in cortical networks. Nat Rev Neurosci 2009;10(2):113–25. DOI: 10.1038/nrn2558

Buzsáki G, Draguhn A. Neuronal Oscillations in Cortical Networks. Science 2004: 304 (5679), 1926-9. DOI:10.1126/science.1099745

Carandini M. Amplification of trial-to-trial response variability by neurons in visual cortex. PLoS Biol 2004;2(9):E264. DOI: 10.1371/journal.pbio.0020264

Druckmann S, Chklovskii DB. Neuronal circuits underlying persistent representations despite time varying activity. Curr Biol 2012;22:2095–103. DOI: 10.1016/j.cub.2012.08.058

Dürig F, Albarracín AL, Farfán FD, Felice CJ. Design and construction of a photoresistive sensor for monitoring the rat vibrissal displacement. J Neurosci Methods 2009;180(1):71–6. DOI: 10.1016/j.jneumeth.2009.02.020

Durstewitz D, Deco G. Computational significance of transient dynamics in cortical networks. Eur J Neurosci 2008;27(1):217–27. DOI: 10.1111/j.1460-9568.2007.05976.x

Farfán FD, Albarracín AL, Felice CJ. Neural encoding schemes of tactile information in afferent activity of the vibrissal system. J Comput Neurosci. 2013;34(1):89-101. DOI: 10.1007/s10827-012-0408-6.

Flandrin P, Rilling G, Goncalves P. Empirical mode decomposition as a filter bank. IEEE Signal Process Lett. 2004;11(2):112–4. DOI: 10.1109/LSP.2003.821662

Haider B, Duque A, Hasenstaub AR, Yu Y, McCormick DA. Enhancement of visual responsiveness by spontaneous local network activity in vivo. J Neurophysiol. 2007;97(6):4186–202. DOI: 10.1152/jn.01114.2006

Hu M, Liang H. Intrinsic mode entropy based on multivariate empirical mode decomposition and its application to neural data analysis. Cogn Neurodyn. 2011;5(3):277-84. DOI: 0.1007/s11571-011-9159-8

Hu M, Liang H. Noise-assisted instantaneous coherence analysis of brain connectivity. Comput Intell Neurosci. 2012;2012:275073. DOI: 10.1155/2012/275073

Hu M, Liang H. Search for information-bearing components in neural data. PLoS One. 2014;16;9(6):e99793. DOI: 10.1371/journal.pone.0099793

Huang NE, Shen Z, Long SR, Wu MC, Shih HH, Zheng Q, et al. The empirical mode decomposition and the Hilbert spectrum for nonlinear and non-stationary time series analysis. Proc R Soc London Ser A Math Phys Eng Sci 1998;454:903–5. DOI: 10.1098/rspa.1998.0193

Huang JR, Fan SZ, Abbod MF, Jen KK, Wu JF, Shieh JS. Application of multivariate empirical mode decomposition and sample entropy in EEG signals via artificial neural networks for interpreting depth of anesthesia. Entropy. 2013;15(9):3325–39. DOI: 10.3390/e15093325

Klampfl S, David SV, Yin P, Shamma SA, Maass W. A quantitative analysis of information about past and present stimuli encoded by spikes of A1 neurons. J Neurophysiol. 2012;108(5):1366–80. DOI: 10.1152/jn.00935.2011

Laurent G. 1996. Dynamical representation of odors by oscillating and evolving neural assemblies. Trends Neurosci. 1996;19(11):489-96. DOI: 10.1016/S0166-2236(96)10054-0

Liang H, Bressler SL, Desimone R, Fries P. Empirical mode decomposition: a method for analyzing neural data. Neurocomputing. 2005a;65,801-7. DOI:10.1016/j.neucom.2004.10.077

Liang H, Bressler SL, Buffalo EA, Desimone R, Fries P. Empirical mode decomposition of field potentials from macaque V4 in visual spatial attention. Biological cybernetics. 2005b; 92:380-92. DOI 10.1007/s00422-005-0566-y

Luczak A, Barthó P, Marguet SL, Buzsáki G, Harris KD. Sequential structure of neocortical spontaneous activity in vivo. Proc Natl Acad Sci U S A. 2007;104(1):347–52. DOI: 10.1073/pnas.0605643104

Mandic DP, Rehman N, Wu Z, Huang NE. Empirical mode decomposition-based time-frequency analysis of multivariate signals: The power of adaptive data analysis. IEEE Signal Process Mag. 2013;30(6):74–86. DOI: 10.1109/MSP.2013.2267931

Naik G, Selvan S, Nguyen H. Single-Channel EMG Classification With Ensemble-Empirical-Mode-Decomposition-Based ICA for Diagnosing Neuromuscular Disorders. IEEE Trans Neural Syst Rehabil Eng. 2015;4320(c). DOI: 10.1109/TNSRE.2015.2454503

Niederreiter H. Random number generation and Quasi-Monte Carlo methods. Encycl. Actuar. Sci. Philadelphia: Society for Industrial and Applied Mathematic. 1992. DOI: 10.1137/1.9781611970081

Okun M, Yger P, Marguet SL, Gerard-Mercier F, Benucci A, Katzner S, et al. Population rate dynamics and multineuron firing patterns in sensory cortex. J. Neurosci. 2013;32(48):17108–19. DOI:10.1523/JNEUROSCI.1831-12.2012.

Okun M, Steinmetz NA, Cossell L, Iacaruso MF, Ko H, Barthó P, et al. Diverse coupling of neurons to populations in sensory cortex. Nature. 2015; 521(7553):511-5 DOI: 10.1038/nature14273

Pardey J, Roberts S, Tarassenko L. A review of parametric modelling techniques for EEG analysis. Med Eng Phys. 1996;18(1):2–11. DOI: 10.1016/1350-4533(95)00024-0

Petersen CC, Hahn TT, Mehta M, Grinvald A, Sakmann B. Interaction of sensory responses with spontaneous depolarization in layer 2/3 barrel cortex. Proc Natl Acad Sci U S A. 2003;100(23):13638–43. DOI: 10.1073/pnas.2235811100

Phinyomark A, Limsakul C, Phukpattaranont P. A Novel Feature Extraction for Robust EMG Pattern Recognition. J Comput. 2009;1(1):71–80. DOI: 0912.3973

Pizá ÁG, Farfán FD, Albarracín AL, Ruiz GA, Felice CJ. Discriminability measures and time–frequency features: An application to vibrissal tactile discrimination. J Neurosci Methods.; 2014;233:78–88. DOI: 10.1016/j.jneumeth.2014.06.007

Rehman N, Mandic DP. Multivariate empirical mode decomposition. Proc R Soc A Math Phys Eng Sci . 2010;466:1291–302. DOI: 10.1098/rspa.2009.0502

Rehman N, Mandic DP. Filter bank property of multivariate empirical mode decomposition. IEEE Trans Signal Process. 2011;59(5):2421–6. DOI: 10.1109/TSP.2011.2106779

Rilling G, Flandrin P, Goncalves P. on Empirical Mode Decomposition and Its Algorithms. IEEEEURASIP Work Nonlinear Signal Image Process NSIP. 2003;3:8–11. DOI: 10.1140/epjnbp/s40366-014-0014-9

Safaai H, von Heimendahl M, Sorando JM, Diamond ME, Maravall M. Coordinated population activity underlying texture discrimination in rat barrel cortex. J Neurosci. 2013;33(13):5843–55. DOI:10.1523/JNEUROSCI.3486-12.2013

Shamir M, Sompolinsky H. Nonlinear population codes. Neural Comput. 2004;16(6):1105-36. DOI: 10.1162/089976604773717559

Theunissen F, Miller JP. Temporal encoding in nervous systems: A rigorous definition. J Comput Neurosci. 1995;2(2):149–62. DOI: 10.1007/BF00961885

Zhan Y, Halliday D, Jiang P, Liu X, Feng J. Detecting time-dependent coherencebetween non-stationary electrophysiological signals – A combined statisticaland time–frequency approach. J Neurosci Methods 2006;156(1–2):322–32. DOI: 10.1016/j.jneumeth.2006.02.013

ZhaohuaW, Huang NE. Ensemble Empirical Mode Decomposition : A Noise Assisted Data Analysis Method. Adv Adapt Data Anal. 2009;1(1):1–41. DOI: 10.1142/S1793536909000047